Microelectronics Reliability 52 (2012) 2875–2879

Contents lists available at SciVerse ScienceDirect

Microelectronics Reliability

journal homepage: www.elsevier.com/locate/microrel

Impact of high-power stress on dynamic ON-resistance of high-voltage GaN HEMTs

Donghyun Jin *, Jesús A. del Alamo

Microsystems Technology Laboratories, Massachusetts Institute of Technology, 60 Vassar St., Rm. 39-567, Cambridge, MA 02139, United States

ARTICLE INFO

Article history:
Received 1 July 2012
Received in revised form 24 August 2012
Accepted 27 August 2012
Available online 19 September 2012

ABSTRACT

We have investigated the impact of high-power (HP) stress on the dynamic ON-resistance (R_{ON}) in high-voltage GaN High-Electron-Mobility Transistors (HEMTs). We use a newly proposed dynamic R_{ON} measurement methodology which allows us to observe R_{ON} transients after an OFF-to-ON switching event from 200 ns up to any arbitrary length of time over many decades. We find that HP-stress results in much worsened dynamic R_{ON} especially in the sub-ms range with minor changes on a longer time scale. We attribute this to stress-induced generation of traps with relatively short time constants. These findings suggest that accumulated device operation that reaches out to the HP state under RF power or hard-switching conditions can result in undesirable degradation of dynamic R_{ON} on a short time scale.

1. Introduction

In the last decade, GaN Field-Effect Transistors have emerged as a promising disruptive technology with great potential for both power electronics and high power microwave applications. This is due to the outstanding electrical properties of the AlGaN/GaN system. For instance, the high breakdown electric field and high sheet electron density attainable in GaN heterostructures promise better than three orders of magnitude ON-resistance/breakdown-voltage trade-off over conventional Si power switching devices [1].

In spite of great recent progress in device fabrication and material growth technologies, electrical reliability still remains a key challenge that prevents the wide deployment of this technology [2,3]. A particular concern is the so-called dynamic ON-resistance (R_{ON}). This refers to a condition in which after an OFF–ON switching event, R_{ON} of the transistor remains high for a certain period of time [3–5]. This is also known as current collapse and greatly affects the use of these devices in power electronics and RF power applications [6]. The detailed physics of dynamic R_{ON} are not completely understood [7]. Much less understanding exists regarding the impact of electrical stress on dynamic R_{ON} [8].

Towards the goal of achieving fundamental understanding of this problem, we have recently developed a new dynamic R_{ON} measurement technique that allows the observation of R_{ON} transients after a switching event over a time period that spans many decades [9]. Using this technique, we study here the impact of high-power (HP) stress on dynamic R_{ON}. We find that HP-stress results in much worsened dynamic R_{ON} in the sub-ms range, that is, R_{ON} increases several fold in a short time scale after an OFF–ON switching event. This occurs as a result of the stress-induced creation of traps with relatively short time constants. On a longer time scale, negligible degradation of dynamic R_{ON} is observed. This suggests that accumulated device operation in the HP state, such as under hard-switching conditions in power switching applications or through an expanded RF load line in RF power amplifier applications at high frequency, can result in undesirable degradation of dynamic R_{ON}. Our results highlight the importance of characterizing electrically stress-induced dynamic R_{ON} and current collapse over very short time scales.

2. Experiments

In this study, we have characterized research prototype AlGaN/GaN HEMTs from an industrial partner fabricated on a heterostructure that has been grown by MOCVD on SiC. The heterostructure includes a GaN cap and an AlN spacer between the AlGaN barrier and the GaN channel. The devices feature an integrated field plate and a source-connected field plate and exhibit a breakdown voltage higher than 200 V. We have stressed these devices in the high-power state with V_{GS} = 2 V ($I_D \approx 0.6$ A/mm) and V_{DS} = 20 V at room temperature which generates a power level of around 12 W/mm. The channel temperature during the stress is estimated to be around 380 °C. This is a very harsh stress condition designed to accelerate the rate of degradation. We interrupt the stress every minute and characterize the evolution of important DC figures of merits such as R_{ON}, maximum drain current (I_{DMAX}), and gate leakage current (I_{GOFF}) using a benign characterization suite [2]. Dynamic R_{ON} is investigated using a recently proposed methodology [9] in which R_{ON} recovery transients originating from an OFF-to-ON switching event are recorded

* Corresponding author.
E-mail address: jinnara@mit.edu (D. Jin).

0026-2714/$ - see front matter © 2012 Elsevier Ltd. All rights reserved.
http://dx.doi.org/10.1016/j.microrel.2012.08.023

from 200 ns to any arbitrary length of time. This is accomplished by combining measurements using an Auriga AU4750 pulsed IV system and an Agilent B1500A semiconductor device analyzer. In both cases, synchronous switching of V_{GS} and V_{DS} is performed. In the pulsed IV system, successive switching from an OFF-state quiescent (Q) bias to an ON state given by V_{GS} = 1 V and V_{DS} between 0.05 and 1.2 V has been performed to measure the linear drain current. The dynamic value of R_{ON} can be extracted from the slope of I_D vs. V_{DS} at different times in the transient from 200 ns up to 3 ms. In the B1500A, the synchronous pulsed mode completes this R_{ON} transient from 3 ms to any arbitrary time. We have applied this method to five identical test devices fabricated on the same chip before and after HP-stress times of 0, 10, 20, 30 and 40 mins.

Fig. 1 plots the time evolution of DC R_{ON} and I_{DMAX} normalized to their initial values as well as I_{GOFF} as a function of stress time for the sample that was stressed for 40 min. The device shows quite robust characteristics up to 30 min. Beyond this point, significant degradation takes place in R_{ON} and I_{DMAX} while a minor increase in I_{GOFF} is observed. The degradation in R_{ON} and I_{DMAX} are mirror images of each other, suggesting a common origin. The samples stressed for 10, 20 and 30 mins exhibit very minor degradation in their DC R_{ON} and I_{DMAX} values, consistent with the results of Fig. 1.

Fig. 2 shows R_{ON} recovery transients from 200 ns up to 200 s for all devices after an OFF-state pulse with $V_{GSQ} = -10$ V and V_{DSQ} = 50 V. From 200 ns up to 3 ms, R_{ON} is continuously being measured at V_{GS} = 1 V and $V_{DS} \leqslant 1.2$ V with a duty cycle of 10% in the pulsed IV system. During the rest of time up to 200 s, R_{ON} is being measured using the I-V time sampling mode in the semiconductor device analyzer after an identical OFF–ON state switching (single pulse) has been applied. In a virgin device, after this switching event, R_{ON} at 200 ns is about 36% higher than in DC (R_{ON-DC}) and recovers back within ∼10 ms. After HP stress, dynamic R_{ON} at 200 ns increases but the recovery takes place on a similar time scale. After 40 min of stress time, the dynamic R_{ON} at 200 ns dramatically increases more than tenfold over R_{ON-DC}. This is very problematic for both power switching and RF applications.

Fig. 3 shows dynamic R_{ON} (R_{ON}/R_{ON_DC}) at 200 ns, 10 µs and 10 ms as well as $R_{ON\_DC}/R_{ON\_DC\_virgin}$ (R_{ON_DC} value in the virgin device) as a function of stress time in a semilog scale. This graph leaves clear how dynamic R_{ON} increases greatly between 30 and 40 min of stress but only on a time scale in the µs range. Beyond

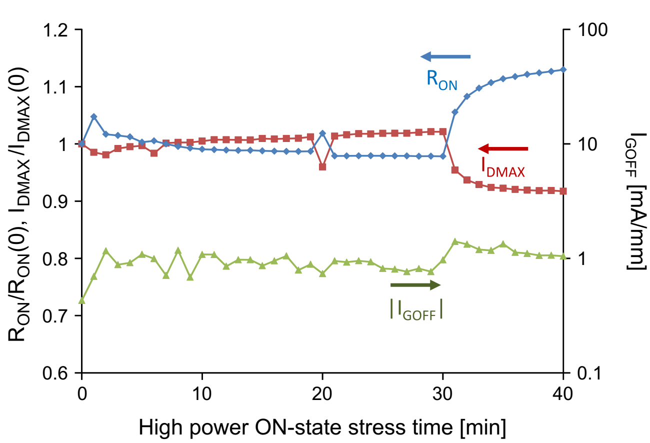

Fig. 1. Time evolution of DC R_{ON}, I_{DMAX} (normalized to their initial values) and $|I_{GOFF}|$ during a constant HP-state stress in GaN HEMTs. R_{ON} is defined by the inverse of the linear drain current measured at V_{GS} = 1 V and V_{DS} = 0.5 V and I_{DMAX} is defined at V_{GS} = 2 V and V_{DS} = 8 V. I_{GOFF} is the gate leakage current measured at $V_{GS} = -5$ V and V_{DS} = 0.1 V. The stress conditions are V_{GS} = 2 V and V_{DS} = 20 V. Up to 30 min of stress, the device characteristics show minor changes. Beyond 30 min, prominent degradation in both R_{ON} and I_{DMAX} and minor one in $|I_{GOFF}|$ are observed.

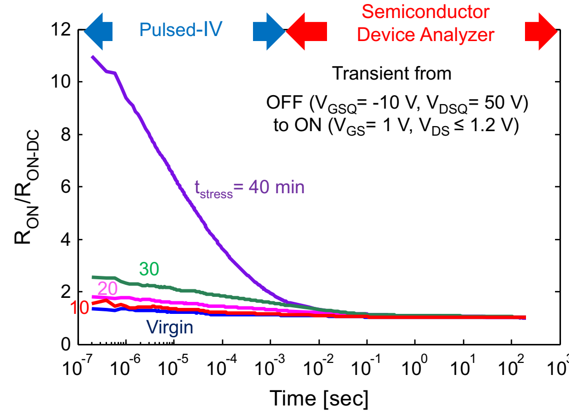

Fig. 2. Dynamic R_{ON} transients from 200 ns up to 200 s after OFF ($V_{GSQ} = -10$ V, V_{DSQ} = 50 V) to ON (V_{GS} = 1 V and $V_{DS} \leqslant 1.2$ V) switching event in different samples that have been subject to different HP-state stress periods ranging from 0 to 40 min. Up to 30 min of stress, minor changes in dynamic R_{ON} are observed. After 40 min of stress, there is a more than 10-fold increase in dynamic R_{ON}. Very fast R_{ON} recovery in the ms range is observed in all cases.

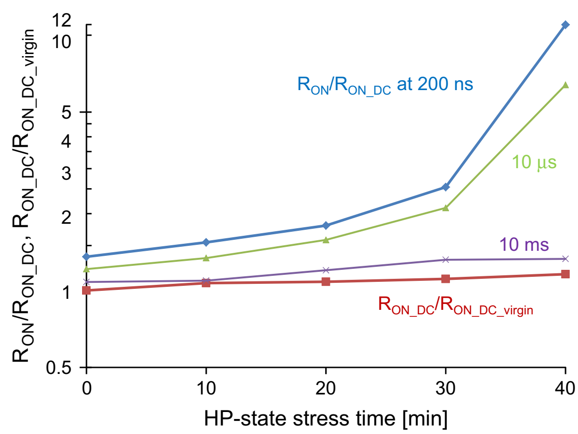

Fig. 3. Normalized dynamic R_{ON} (R_{ON}/R_{ON_DC}) of Fig. 2 at different times (200 ns, 10 µs, and 10 ms) and $R_{ON\_DC}/R_{ON\_DC\_virgin}$ (R_{ON_DC} value in the virgin device) as a function of HP-state stress time in a semilog scale. Dynamic R_{ON} mostly increases in a time range from 200 ns up to a few ms. $R_{ON\_DC}/R_{ON\_DC\_virgin}$ shows small increase up to 16% in comparison to dynamic R_{ON} suggesting minor permanent (non-transient) degradation.

10 ms or so, few changes are observed. In addition, $R_{ON\_DC}/R_{ON\_DC\_virgin}$ shows a small increase up to 16% in comparison to dynamic R_{ON} suggesting minor permanent (non-transient) degradation. These findings highlight the importance of selecting an appropriate time scale for the study of dynamic R_{ON} and current collapse in GaN HEMTs after electrical stress.

In order to understand the physical origin of these prominent transients, we have analyzed the time domain R_{ON} data by fitting it with a sum of exponentials (see inset in Fig. 4) [10]. 20 different time constants per time decade equally distributed in a logarithmic time scale were used in the fit of every transient. The amplitude of the various components as a function of their respective time constants is shown in Fig. 4. It is clear that after 40 min of stress time, fast transients emerge with time constants in the µs to ms range. In contrast, negligible changes occur in the long time constant domain.

Dynamic R_{ON} measurements at different ambient temperatures (T) have been performed with the goal of illuminating the physical origin of these transients. The inset of Fig. 5 shows R_{ON} transients at T between 25 °C and 150 °C for the sample that has been subject to 40 min HP stress. As the temperature increases, R_{ON_DC} increases

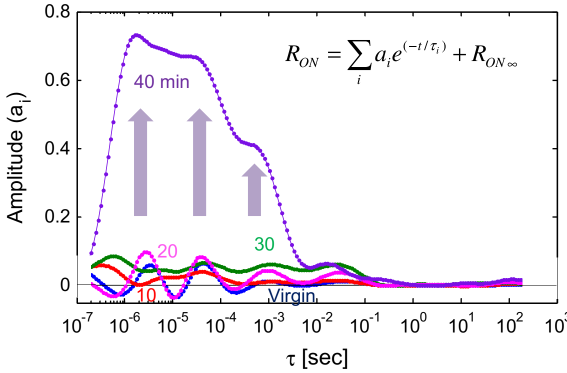

Fig. 4. Time-constant spectra for R_{ON} transients of Fig. 2. A sum of exponential terms with time constant ranging from 200 ns to 200 s is used to fit the measurement data. The equation used for fitting is indicated in the inset. The fit yields the a_i coefficient corresponding to each time constant τ_i. These data reveal that after 40 min of stress, there is a prominent increase of the magnitude of transients with short time constants.

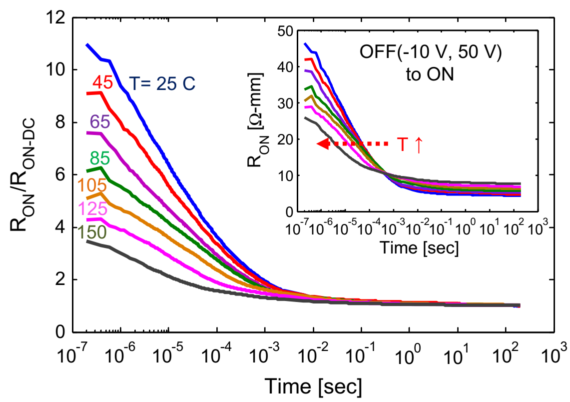

Fig. 5. R_{ON}/R_{ON_DC} transients at different temperatures between 25 °C and 150 °C for $V_{GSQ} = -10$ V and $V_{DSQ} = 50$ V after 40 min HP stress. The inset shows the absolute value of the R_{ON} transient. As the temperature goes up, the dominant transients are substantially accelerated. This suggests that the transients are due to generated traps.

due to a reduction in mobility. R_{ON} at 200 ns, on the other hand, decreases as electron trapping is mitigated at high temperature. This is more clearly seen in Fig. 5 that shows the normalized value of R_{ON} over the R_{ON_DC} value. As the temperature increases, trapping is less severe and the recovery transient is considerably accelerated.

Fig. 6 exhibits the time constant spectra extracted from R_{ON} transients over a wide temperature range from −55 °C to 150 °C including transients from Fig. 5. Arrows with different colors identify the evolution of individual time constant peaks across temperatures. Most of the time constants are seen to shorten as temperature increases which suggests that they originate from thermally assisted electron detrapping from conventional traps (as opposed to traps that communicate with the channel through a tunneling process [9,11,12]).

The evolution of the dominant time constants with temperature is depicted in an Arrhenius plot in Fig. 7. The size of the symbols is proportional to the magnitude of the peak in the time constant spectra of Fig. 6. The color of the symbols is also consistent with the arrows in Fig. 6. The thermally activated behavior for the time constants that is obtained allows us to conclude that conventional traps are responsible for the increase in dynamic R_{ON}. Fig. 7 reveals that the dominant trap energy levels that have been created as a result of electrical stress have ionization energies of 0.31, 0.45, 0.53 and 0.57 eV. Traps with low energy levels such as 0.23, 0.31,

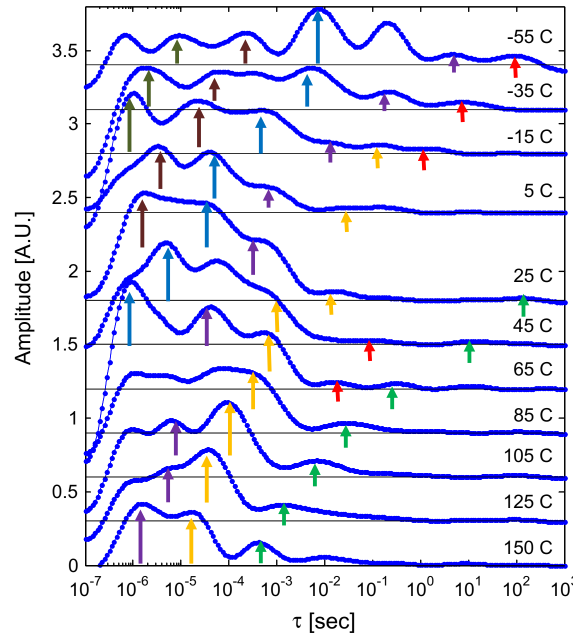

Fig. 6. Time-constant spectra for R_{ON} transients for temperatures between −55 °C and 150 °C including the transients in Fig. 5. Arrows with different colors distinguish individual time constant peaks at different temperatures. Most of them move towards shorter time constants as the temperature increases indicating a thermally activated behavior . (For interpretation of the references to colour in this figure legend, the reader is referred to the web version of this article.)

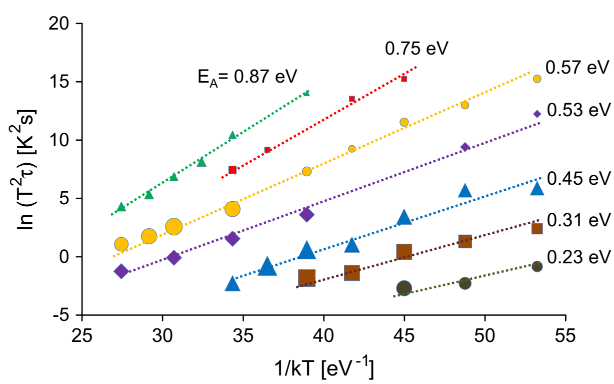

Fig. 7. Arrhenius plot of time constant spectra from Fig. 6. The size of the symbols is proportional to the height of the time constant peaks and the color of them matches that of the arrows in Fig. 6. The dominant trap energy levels are located at 0.31, 0.45, 0.53 and 0.57 eV below the conduction band edge most likely in the AlGaN barrier. These are the traps that are responsible for the dramatic increase in dynamic R_{ON} that is observed in the short time scale. (For interpretation of the references to colour in this figure legend, the reader is referred to the web version of this article.)

and 0.45 eV appear to have been generated as a result of the HP-stress whereas deeper traps already existed in the virgin sample but their density seems to have increased [9]. The observed traps are presumed located below the conduction band edge of the AlGaN barrier inside its body or at the surface. Similar trap energy levels have also been reported in similar structures after electrical stress by other authors [13,14].

3. Discussion

Through the HP-stress test, GaN HEMTs experience not only very high temperature in the channel region but also a high electric field which can potentially produce copious amounts of hot electrons [15]. These can create the damage that is behind the observed degradation of dynamic R_{ON}. The roles of V_{DS} and temperature in the degradation of dynamic R_{ON} during HP stress can be separated by performing tests at different bias conditions. In Fig. 8, we show the evolution of dynamic R_{ON} normalized to its DC value after an HP-stress experiment at a higher V_{DS} of 30 V but lower power level around 9 W/mm (by reducing the DC stress current). The channel temperature is expected to be lowered down to 291 °C. Even after only 3 min of this HP stress, the dynamic R_{ON} at 200 ns in response to an OFF to ON switching event (same conditions as earlier in this paper) increases 5-fold over the DC value, as shown in Fig. 8. When compared with the much smaller R_{ON}/R_{ON_DC} increase after 20 min of HP stress at a lower V_{DS} of 20 V and higher power level around 12 W/mm (also shown in the graph), this result suggests that HP stress at higher V_{DS} induces greater dynamic R_{ON} degradation. Under these new conditions, the R_{ON} transients show fast recovery in the sub-ms range suggesting the same physical origin of the created traps in both experiments.

Our recent studies of dynamic R_{ON} in AlGaN/GaN high-voltage HEMTs suggest that epitaxial growth conditions greatly matter [9]. Here, we illustrate how different growth protocols of otherwise identical structures also yield markedly different robustness of dynamic R_{ON} to high power electrical stress. For this purpose, we have tested devices made from wafers grown by a different epi supplier (denoted here as "epi supplier II" in contrast with the results presented up to now in this paper on samples from a different "epi supplier I"). The two wafers were processed into devices in the same lot. Fig. 9 shows the time evolution of normalized DC R_{ON} and I_{DMAX} as well as $|I_{GOFF}|$ during a constant HP-stress experiment on a device from a wafer grown by epi-supplier II. The stress conditions are identical to those of Fig. 1 (V_{GS} = 2 V and V_{DS} = 20 V), but the stress period is lengthened to 2 h. In spite of this longer stress time, in the epi-supplier II sample, in contrast to the epi-supplier I case, negligible degradation is observed in R_{ON} and I_{DMAX} during this stress test. A large increase of $|I_{GOFF}|$ is observed but we find this to be fully recoverable under sufficient visible-light illumination.

Dynamic R_{ON} transients after identical OFF (V_{GSQ} = −10 V, V_{DSQ} = 50 V) to ON switching events were also measured before and after 2 h HP-stress test in the epi-supplier II sample and are shown in Fig. 10. Compared with the intrinsic dynamic R_{ON} transient

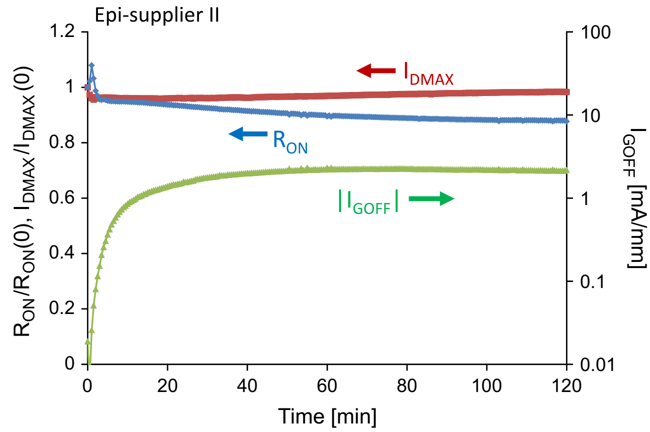

Fig. 9. Time evolution of normalized DC R_{ON}, I_{DMAX} and $|I_{GOFF}|$ in a constant HP-state stress in devices made from a different epi-supplier sample (denoted as epi-supplier II). The stress conditions are those of Fig. 1 (V_{GS} = 2 V, V_{DS} = 20 V) but the stress time is extended to 2 h. In the epi-supplier II sample, there is no prominent permanent degradation in R_{ON}, I_{DMAX} and $|I_{GOFF}|$. The large increase of $|I_{GOFF}|$ is fully recoverable under sufficient illumination of visible light.

characteristic of the virgin epi-supplier II sample, there is only a minor increase in the dynamic R_{ON} observed even after the 2 h HP stress. This is also much less than the dynamic R_{ON} transient observed in the sample from epi-supplier I after much shorter stress under the same conditions. This result suggests that epi-supplier II devices are more robust to HP-state stress than those of epi-supplier I. A detailed study of the origin of this is beyond the scope of this paper. However, two possible explanations are apparent. The different buffer design in the two structures affects the thermal conductance of the substrate. In fact, the thermal resistance of the device from epi-supplier II is estimated to be lower than 10 °C/W which is one third of that of the equivalent epi-supplier I sample. A much lower channel temperature during the same HP stress should be less harmful to the device. In addition, the epi-supplier II sample has a greater concentration of long-time constant traps than the epi-supplier I sample [9]. When these traps held electrons, they alleviate the electric field profile inside the device [16]. For the same V_{DS} bias condition, a device structure with a greater concentra-

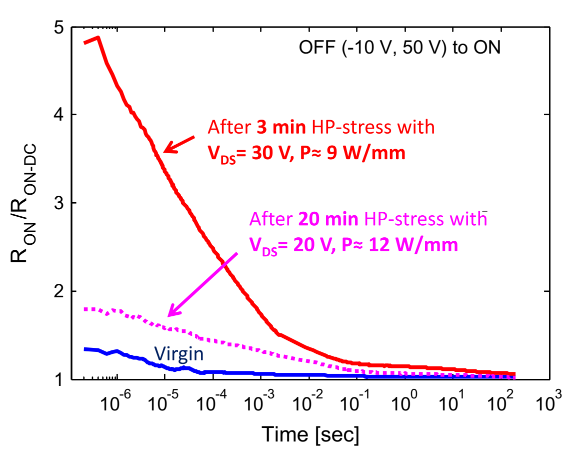

Fig. 8. Dynamic R_{ON} transients after OFF (V_{GSQ} = −10 V, V_{DSQ} = 50 V) to ON switching event for samples subjected to HP-state stress under different conditions. The red solid line indicates a very large increase of dynamic R_{ON} up to 5-fold R_{ON-DC} at 200 ns only after 3 min HP stress at V_{DS} = 30 V (P = 9 W/mm). In comparison with the R_{ON}/R_{ON-DC} increase after 20 min HP stress at lower V_{DS} of 20 V and higher P level of 12 W/mm in pink dashed line, this result suggests that HP stress at higher V_{DS} promotes greater dynamic R_{ON} degradation. In all cases, a very fast R_{ON} recovery down to the ms range is observed. (For interpretation of the references to colour in this figure legend, the reader is referred to the web version of this article.)

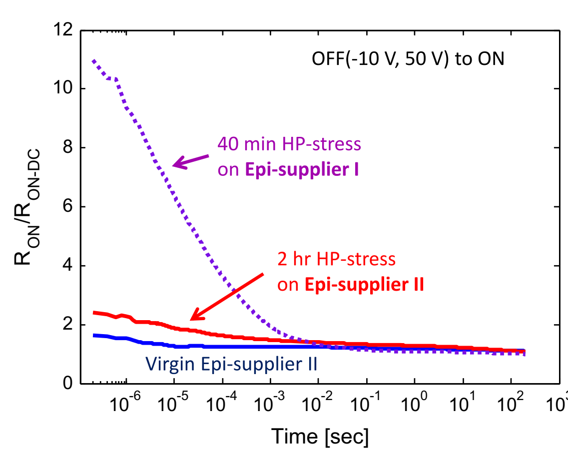

Fig. 10. Dynamic R_{ON} transient after an OFF (V_{GSQ} = −10 V, V_{DSQ} = 50 V) to ON switching event on epi-supplier II sample before and after 2 h HP stress at V_{GS} = 2 V and V_{DS} = 20 V ($P \approx$ 12 W/mm). In contrast to the large degradation of dynamic R_{ON} in epi-supplier I device after the 40 min HP-stress (purple dashed line), there is only a minor increase of dynamic R_{ON} observed after 2 h HP stress in epi-supplier II sample. (For interpretation of the references to colour in this figure legend, the reader is referred to the web version of this article.)

tion of traps might then be more robust to hot-electron induced degradation.

4. Conclusions

We have experimentally observed a large increase in dynamic R_{ON} on a short-time scale after high-power electrical stress of GaN HEMTs. The cause is attributed to the formation of shallow traps inside the AlGaN barrier or at its surface. A rich spectrum of traps with different binding energies has been identified. This work suggests that prolonged device operation of GaN HEMTs under RF power conditions (in microwave applications) or under hard-switching conditions (in power management) can result in an undesirable increase of dynamic R_{ON} on a very short time scale.

Acknowledgments

This research is supported in part by U.S. Department of Energy in the context of the ARPA-E ADEPT program, by the Semiconductor Research Corporation and by the DRIFT MURI under an ONR Grant.

References

[1] Briere MA. GaN on Si based power devices: an opportunity to significantly impact global energy consumption. In: 25th compound semiconductor manufacturing technology conference, May 2010. p. 221.
[2] del Alamo JA, Joh J. GaN HEMT reliability. Microelectron Reliab 2009;49(9):1200–1206.
[3] Wuerfl J et al. Reliability issues of GaN based high voltage power devices. Microelectron Reliab 2011;51(9):1710–6.
[4] Saito W et al. Suppression of dynamic on-resistance increase and gate charge measurements in high-voltage GaN-HEMTs with optimized field-plate structure. IEEE Trans Electron Dev 2007;54(8):1825–30.
[5] Chu R et al. 1200-V normally off GaN-on-Si field-effect transistors with low dynamic on-resistance. IEEE Electron Dev Lett 2011;32(5):632–4.
[6] Binari SC et al. Trapping effects in GaN and SiC microwave FETs. Proc IEEE 2007;90(6):1048–58.
[7] Faqir M et al. Mechanisms of RF current collapse in AlGaN-GaN high electron mobility transistors. IEEE Trans Electron Dev 2008;8(2):240–7.
[8] Meneghesso G et al. Current collapse and high-electric-field reliability of unpassivated GaN/AlGaN/GaN HEMTs. IEEE Trans Electron Dev 2006;53(12):2932–41.
[9] Jin D, del Alamo JA. Mechanisms responsible for dynamic ON-resistance in GaN high-voltage HEMTs. In: 24th IEEE international symposium on power semiconductor devices and ICs, June 2012. p. 333–6.
[10] Joh J, del Alamo JA. A current-transient methodology for trap analysis for GaN high electron mobility transistors. IEEE Trans Electron Dev 2011;58(1):132–40.
[11] Vitusevich SA et al. Low-frequency noise in AlGaN/GaN HEMT structures with AlN thin film layer. Phys Stat Sol (c) 2006;3(6):2329–32.
[12] Fleetwood DM et al. Estimating oxide-trap, interface-trap, and border-trap charge densities in metal–oxide–semiconductor transistors. Appl Phys Lett 1994;64(15):1965–7.
[13] Arehart AR et al. Spatially-discriminating trap characterization methods for HEMTs and their application to RF-stressed AlGaN/GaN HEMTs. In: IEDM techology digest; December 2010. p. 464–7.
[14] Sozza A et al. Evidence of traps creation in GaN/AlGaN/GaN HEMTs after a 3000 h on-state and off-state hot-electron stress. In: IEDM techology digest, December 2005. p. 589–93.
[15] Meneghini M et al. Impact of hot electrons on the reliability of AlGaN/GaN high electron mobility transistors. In: International reliability physics symposium, April 2012. p. 2C2.1–2C2.5.
[16] Demirtas S, del Alamo JA. Effect of trapping on the critical voltage for degradation in GaN high electron mobility transistors. In: 2010 International reliability physics symposium, May 2010; p. 134–8.